

# RSC Advances



This is an *Accepted Manuscript*, which has been through the Royal Society of Chemistry peer review process and has been accepted for publication.

*Accepted Manuscripts* are published online shortly after acceptance, before technical editing, formatting and proof reading. Using this free service, authors can make their results available to the community, in citable form, before we publish the edited article. This *Accepted Manuscript* will be replaced by the edited, formatted and paginated article as soon as this is available.

You can find more information about *Accepted Manuscripts* in the [Information for Authors](#).

Please note that technical editing may introduce minor changes to the text and/or graphics, which may alter content. The journal's standard [Terms & Conditions](#) and the [Ethical guidelines](#) still apply. In no event shall the Royal Society of Chemistry be held responsible for any errors or omissions in this *Accepted Manuscript* or any consequences arising from the use of any information it contains.

Cite this: DOI: 10.1039/c0xx00000x

www.rsc.org/xxxxxx

ARTICLE TYPE

## Improved low-temperature activity of La-Sr-Co-O nano-composite for CO oxidation by phase cooperation

Linyun Zhong, Fang Hai, Ping Xiao, Jingping Hong and Junjiang Zhu\*

Received (in XXX, XXX) XthXXXXXXXXXX 20XX, Accepted Xth XXXXXXXXXXXX 20XX

DOI: 10.1039/b000000x

La<sub>0.7</sub>Sr<sub>0.3</sub>-Co-O nano-composite shows stable and improved low-temperature activity for CO oxidation, with temperature for ignition and full CO oxidation at 70 and 174 °C, respectively. Benefitted from the perovskite component, the catalyst shows stable activity during the reaction without appreciable loss after 36 h. Together with the characteristic results from XRD, XPS and TEM, it is inferred that the high activity of La<sub>0.7</sub>Sr<sub>0.3</sub>-Co-O is attributed to its porous structure, optimized Sr substitution, and especially a phase cooperation effect between the perovskite and metal oxides.

Perovskite oxides are attractive material in catalysis and have been widely investigated in recent years because of their unique structures, in which the cation at either A- or B-site can be substituted by a foreign one without destroying the matrix structure, thus the oxidation state of B-site cation and the content of oxygen vacancy can be controlled as desired, offering a feasible way to correlate physicochemical properties with catalytic performances of a material.<sup>1-4</sup> Also, their low-cost, high thermal and hydrothermal stability, straightforward synthesis as well as considerable catalytic performance make them potential material to substitute noble metal catalysts for industrial use.<sup>5-8</sup>

One application of perovskite oxides is for catalytic oxidation removal of CO, which is an unwanted gas produced in automobile exhaust and solid oxide fuel cell (SOFC).<sup>9-12</sup> In contrast to metal oxide or noble metal catalysts, the perovskite oxides need to be performed at a higher temperature. For instance, the temperature of full CO oxidation over LaCoO<sub>3</sub> is near to 200 °C,<sup>13-15</sup> which is far higher than that over Co<sub>3</sub>O<sub>4</sub><sup>16,17</sup> and gold catalysts.<sup>18,19</sup> This limits largely their use in practice. The improvement of low-temperature activity of perovskite oxides for CO oxidation thus is essential before its possible industrialization.

Four strategies have been suggested to improve the catalytic activity of perovskite oxide in literature: the first is to use a suitable preparation method, to generate desired surface properties and compositions;<sup>20,21</sup> the second is to optimize the metals at either A- or B-site, to enhance the physicochemical properties;<sup>22,23</sup> the third is to fabricate the material in nano-sized or porous structure, to increase the surface area and to expose more active site on the surface;<sup>24-26</sup> and the last is to synthesize a multi-phase material, by which synergistic effect between the perovskite and other phases that facilitates the reaction can be

induced.<sup>27-29</sup>

In this work we report a highly active La<sub>0.7</sub>Sr<sub>0.3</sub>-Co-O nano-composite for CO oxidation. This sample has all the virtues mentioned above, that is, optimized A-site cation, nano-sized structure and mixed phases that can induce synergistic effect for the catalytic reactions. As expected it shows improved low-temperature activity for CO oxidation relative to the perovskite (e.g., La<sub>0.7</sub>Sr<sub>0.3</sub>CoO<sub>3</sub>) and the simple oxide (e.g., Co<sub>3</sub>O<sub>4</sub>), with the temperature for ignition and full CO conversion at 70 and 174 °C, respectively. Moreover, the catalyst is stable with no appreciable loss in the activity after reaction for 36 h, showing potential application for oxidation removal of CO in practice.

XRD results of the La-B-O (B = Fe, Co, Ni, Cu) samples show that La-Fe-O and La-Co-O have a relatively good perovskite structure, while La-Ni-O and La-Cu-O exhibit a lot of impurity peaks (see Figure S1 of the supporting information, SI). This indicates that Fe and Co are more suitable metals than Ni and Cu in the formation of oxides with perovskite structure. A possible reason could be that Fe and Co can exist in +3 oxidation state easier than Ni and Cu, which exist mainly in +2 oxidation state, thus facilitating the formation of LaBO<sub>3</sub> perovskite structure from the viewpoint of electroneutrality, since La has +3 and O has -2 oxidation state. In addition, screening tests on CO oxidation over the samples show that La-Co-O is the best catalyst for the reaction (see below, Figure 3A). We thus choose cobalt as objective metal for further investigations.

Figure 1A presents the XRD patterns of the series of cobalt based samples, showing that sample without Sr addition (La-Co-O) has a good perovskite structure, but the structure is gradually destroyed and simple metal oxides, e.g., Co<sub>3</sub>O<sub>4</sub>, appear with the increase of Sr content, indicating that the Sr addition suppressed the formation of perovskite structure. The proportion of Co<sub>3</sub>O<sub>4</sub> increases with the Sr content, as reflected by the intensity ratio of peak at 37° (for Co<sub>3</sub>O<sub>4</sub>) to that at 33° (for LaCoO<sub>3</sub>), which increases from 0 to 1.26 and to 1.44 with the Sr content from 0 to 0.1 and to 0.3, respectively. The perovskite structure is fully collapsed at 70% Sr percentage (i.e., La<sub>0.3</sub>Sr<sub>0.7</sub>-Co-O). The suppressing effect of Sr however can be overcome by supplying sufficient energy to the system. For example, La<sub>0.7</sub>Sr<sub>0.3</sub>CoO<sub>3</sub> with pure perovskite structure can be formed by increasing the calcination temperature to 800 °C with otherwise identical conditions (see Figure 1A). It is noted that the peak at about 2θ = 33° was split, suggesting the formation of two possible perovskite phases: LaCoO<sub>3</sub> and SrCoO<sub>3</sub>, which is similar to results reported

by other authors<sup>30</sup>.

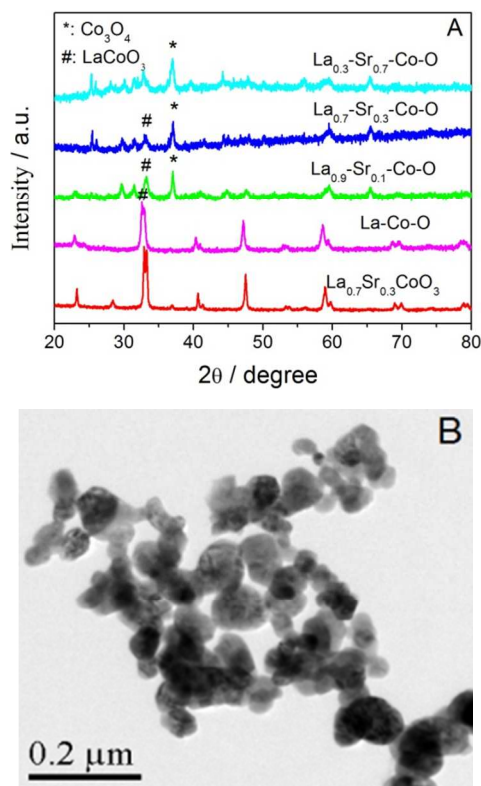


**Figure 1.** (A) Wide-angle XRD patterns for the series of investigated catalysts; (B) Typical TEM image for  $\text{La}_{0.7}\text{Sr}_{0.3}\text{-Co-O}$

Figure 1B presents a typical TEM image for sample  $\text{La}_{0.7}\text{Sr}_{0.3}\text{-Co-O}$ , showing a nano-sized structure, with the average particle size of *ca.* 60 nm. The nano-sized structure is also observed for  $\text{Co}_3\text{O}_4$  and  $\text{LaCoO}_3$  (see Figure S2 of the SI), indicating that the current sol-gel method using ethylene glycol and formic acid as complexing agent is effective for preparing nano-sized oxides.  $\text{N}_2$  physisorption measurements show that the BET (five points) surface areas of these nano-sized La1-x-Srx-Co-O samples are considerable, in the range of 11 - 15  $\text{m}^2 \text{g}^{-1}$ .

For CO oxidation conducted over oxides catalyst the surface oxygen and metal species are two major factors influencing the activity as they are components of the active site. For this XPS measurement, which is a surface-sensitive technique and provides information on the surface elemental compositions and surface chemistry of material, are conducted to supply information for the surface oxygen and cobalt species of the samples. Figure 2 presents the XPS spectra surveyed from Co 2p and O 1s of the samples. For Co 2p the peak area decreases in order of  $\text{Co}_3\text{O}_4 > \text{La}_{0.7}\text{Sr}_{0.3}\text{-Co-O} > \text{La}_{0.7}\text{Sr}_{0.3}\text{CoO}_3$ , indicating that  $\text{La}_{0.7}\text{Sr}_{0.3}\text{CoO}_3$  has the least number of surface cobalt species, due to the enrichment of La and Sr on the surface as justified by the surface (La+Sr)/Co ratio listed in Table 1. In contrast  $\text{La}_{0.7}\text{Sr}_{0.3}\text{-Co-O}$  shows high percentage of surface Co species, with (La+Sr)/Co ratio of 0.65. The higher percentage of exposed surface Co species suggests that there is more active site on the  $\text{La}_{0.7}\text{Sr}_{0.3}\text{-Co-O}$  than that on the  $\text{La}_{0.7}\text{Sr}_{0.3}\text{CoO}_3$ . In order to analyze the surface composition of Co species, the peaks were deconvoluted using XPS peak analysis software (XPS Peak) and the calculated results are listed in Table 1. From literature and our previous

work it is known that the peak fitted at 779.5 and 782.8 eV is assigned to surface  $\text{Co}^{3+}$  and  $\text{Co}^{2+}$ , respectively, and the peak fitted at 789.4 eV is to a satellite peak of  $\text{Co}^{2+}$  species<sup>15,31</sup>. The  $\text{Co}^{3+}/\text{Co}^{2+}$  ratio for  $\text{La}_{0.7}\text{Sr}_{0.3}\text{-Co-O}$  is 1.38, which is lower than that for  $\text{Co}_3\text{O}_4$  and  $\text{La}_{0.7}\text{Sr}_{0.3}\text{CoO}_3$  (1.65 and 1.63, respectively). The low  $\text{Co}^{3+}/\text{Co}^{2+}$  ratio implies that oxygen vacancy is generated and  $\text{Co}_3\text{O}_4$  phase is formed in the sample. From the principle of electroneutrality and the composition of  $\text{Co}_3\text{O}_4$ , it is known that the generation of oxygen vacancy and the formation of  $\text{Co}_3\text{O}_4$  would lead to the presence of  $\text{Co}^{2+}$  species. The closer to unity of  $\text{Co}^{3+}/\text{Co}^{2+}$  ratio might also suggests a easier transformation between  $\text{Co}^{3+}$  and  $\text{Co}^{2+}$  ( $\text{Co}^{3+}[\text{e}^-] \leftrightarrow \text{Co}^{2+}$ ). This is important as catalysis is a redox reaction which requires the redox cycling of the active site. The binding energy of  $\text{Co}^{3+}$  species for  $\text{Co}_3\text{O}_4$  shifts to a higher position relative to that of the other two, possibly due to a different coordinate environment.

**Table 1** Surface compositions of each atom for the samples, determined from XPS spectra

Sample	(La+Sr)/Co	$\text{Co}^{3+}/\text{Co}^{2+}$	$\text{O}_{\text{ads}}/\text{O}_{\text{latt}}$
$\text{Co}_3\text{O}_4$	—	1.65	1.25
$\text{La}_{0.7}\text{Sr}_{0.3}\text{-Co-O}$	0.65	1.38	1.31
$\text{La}_{0.7}\text{Sr}_{0.3}\text{CoO}_3$	1.78	1.63	2.61

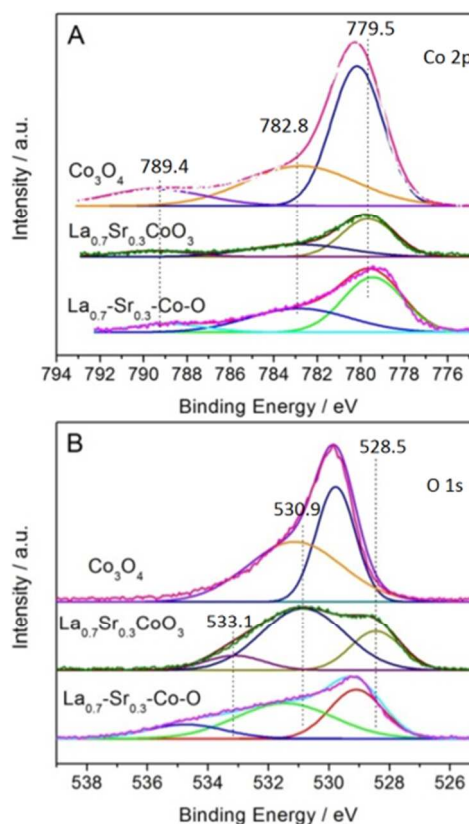


**Figure 2.** XPS spectra surveyed from the (A) Co 2p and (B) O 1s of  $\text{Co}_3\text{O}_4$ ,  $\text{La}_{0.7}\text{Sr}_{0.3}\text{CoO}_3$  and  $\text{La}_{0.7}\text{Sr}_{0.3}\text{-Co-O}$

Similarly, the O 1s spectra was also deconvoluted and the peaks fitted at 528-529 eV and 530-532 eV are assigned to lattice oxygen and oxygen adsorbed on the oxygen vacancy, respectively, Figure 2B.<sup>32</sup> By comparison, it is seen that the peak

fitted for  $\text{La}_{0.7}\text{Sr}_{0.3}\text{Co-O}$  is shifted to a higher position relative to that for  $\text{La}_{0.7}\text{Sr}_{0.3}\text{CoO}_3$ , indicating a more reactive oxygen species (the oxygen is more liberal). From the surface  $O_{\text{ads.}}/O_{\text{latt.}}$  ratio it is seen that the value increases in sequence of  $\text{Co}_3\text{O}_4 < \text{La}_{0.7}\text{Sr}_{0.3}\text{Co-O} < \text{La}_{0.7}\text{Sr}_{0.3}\text{CoO}_3$ . This indicates that the generation of oxygen vacancy, on which adsorbed oxygen ( $O_{\text{ads.}}$ ) is produced, is more feasible in perovskite than that in simple oxide. By comparing with the shift in oxygen binding energy and the  $O_{\text{ads.}}/O_{\text{latt.}}$  ratio of the samples, it is inferred that the  $\text{La}_{0.7}\text{Sr}_{0.3}\text{Co-O}$  sample is composed of perovskite and simple metal oxide, that is, a multi-phase structure. The peak fitted at above 533 eV is suggested to be attributed to the adsorbed oxygen and/or water.<sup>15, 33</sup> The XPS spectra for La 3d, Sr 3d, as well as the Co 2p and O 1s of samples with different Sr contents are presented in Figure S3 of the SI).

$\text{O}_2$ -TPD and  $\text{H}_2$ -TPR measurements are conducted to supply information for the physicochemical properties of oxygen and cobalt atoms. Results are presented in Figure S5A and S5B of the SI, respectively.  $\text{O}_2$ -TPD profiles show that the temperature for oxygen desorption is the lowest (588 °C) for  $\text{La}_{0.7}\text{Sr}_{0.3}\text{Co-O}$ . Considering that this sample has low  $\text{Co}^{3+}/\text{Co}^{2+}$  and  $O_{\text{ads.}}/O_{\text{latt.}}$  ratio, and its composition is in between  $\text{La}_{0.7}\text{Sr}_{0.3}\text{CoO}_3$  and  $\text{Co}_3\text{O}_4$ , the low oxygen desorption temperature must be due to a synergistic effect between the phases that facilitates the oxygen mobility.  $\text{H}_2$ -TPR profiles indicate that the reduction temperature for  $\text{La}_{0.7}\text{Sr}_{0.3}\text{Co-O}$  begins at 240 °C, which is the same as that of  $\text{Co}_3\text{O}_4$  and is lower than that of  $\text{La}_{0.7}\text{Sr}_{0.3}\text{CoO}_3$ . This is acceptable as  $\text{Co}_3\text{O}_4$  is one component of  $\text{La}_{0.7}\text{Sr}_{0.3}\text{Co-O}$  and simple metal oxide normally is more reducible than perovskite oxide. As expected the reduction peak area and the stability of  $\text{La}_{0.7}\text{Sr}_{0.3}\text{Co-O}$  are in between that of  $\text{La}_{0.7}\text{Sr}_{0.3}\text{CoO}_3$  and  $\text{Co}_3\text{O}_4$ , the latter shows the largest reduction peak area and is completely reduced at temperature below 530 °C.

Catalytic tests on the series of La-B-O (B = Fe, Co, Ni, Cu, Zn) oxides show that La-Co-O is the best and La-Zn-O is the worst catalyst for CO oxidation, with an activity order of  $\text{La-Co-O} > \text{La-Cu-O} > \text{La-Ni-O} > \text{La-Fe-O} > \text{La-Zn-O}$ , Figure 3A, indicating that the type of transition metal influences greatly on the CO oxidation activity. The high activity of La-Co-O could be that, on the one hand, La-Co-O with perovskite structure possesses more oxygen vacancy and has better redox ability relative to La-Ni-O and La-Cu-O, which are in mixed metal oxide status, as verified by  $\text{H}_2$ -TPR results (see Figure S5), and on the other hand, the surface oxygen on La-Co-O is more liberal and reactive than that on La-Fe-O, because of the weaker affinity of La-Co-O to surface oxygen.<sup>34</sup>

On preparing active perovskite catalyst for CO oxidation, Dai *et al.* report that  $\text{LaCoO}_3$  fabricated in porous structure shows better activity for CO oxidation than that in the bulk structure due to the improved surface area and physicochemical properties.<sup>14</sup> In this respect we compared the catalytic performances of  $\text{LaCoO}_3$  prepared with and without PMMA template (which is used to create pores inside the structure) for CO oxidation, finding no appreciable change in the activity is observed throughout the reaction (see Figures S2C, S4 and S6 of the SI). This indicates that the herein catalyst has comparable catalytic performances to porous sample, due to its nano-sized structure (see Figure 1B). The nano-sized particles exhibit improved activity for the

reaction similar to that of porous sample.

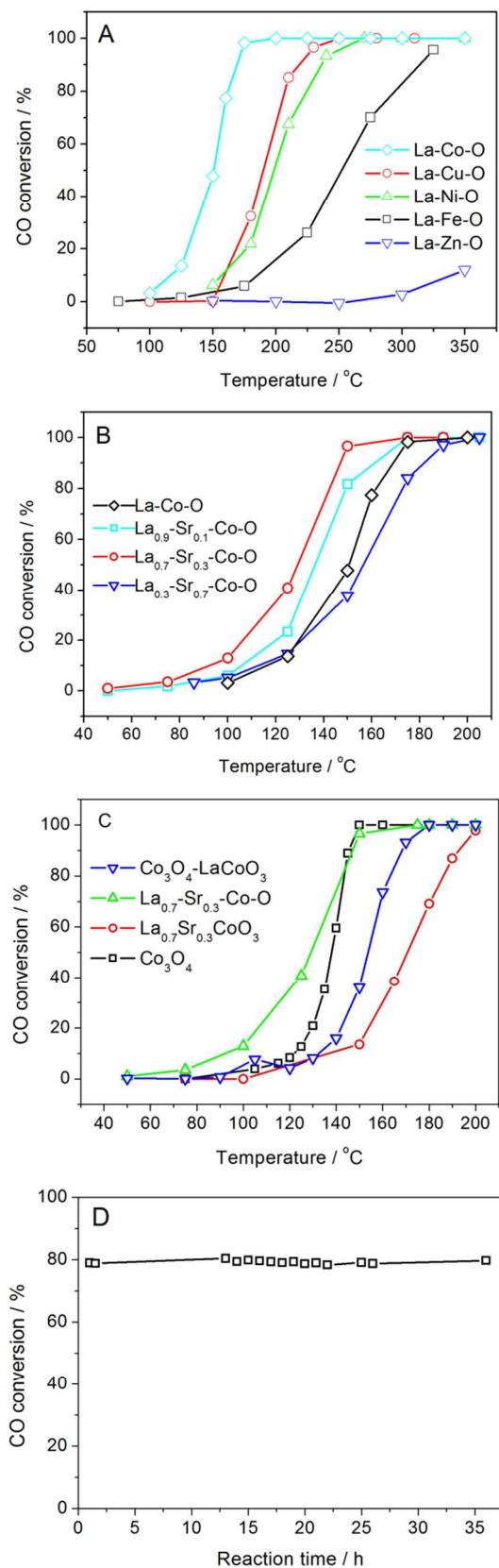


**Figure 3.** CO oxidation over catalysts (A) La-B-O (B = Fe, Co, Ni, Cu, Zn) oxides; (B)  $\text{La}_{1-x}\text{Sr}_x\text{Co-O}$  ( $x = 0, 0.1, 0.3, 0.7$ ); (C)  $\text{Co}_3\text{O}_4$ ,  $\text{La}_{0.7}\text{Sr}_{0.3}\text{CoO}_3$ ,  $\text{La}_{0.7}\text{Sr}_{0.3}\text{Co-O}$  and a mechanically mixed sample  $\text{Co}_3\text{O}_4\text{-LaCoO}_3$ .

La<sub>0.7</sub>Sr<sub>0.3</sub>CoO<sub>3</sub>; (D) the long-time stability of La<sub>0.7</sub>-Sr<sub>0.3</sub>-Co-O composite at reaction temperature 140 °C.

Further optimizations by substitution of Sr<sup>2+</sup> for La<sup>3+</sup> show that sample with Sr<sup>2+</sup> molar percentage of 30%, *i.e.*, La<sub>0.7</sub>-Sr<sub>0.3</sub>-Co-O, is more favorable for the reaction, Figure 3B. The reason could be due to the segregation of simple metal oxide, *e.g.*, Co<sub>3</sub>O<sub>4</sub>, in the sample induced by the Sr addition. The cooperation between Co<sub>3</sub>O<sub>4</sub> and the perovskite oxide results in a synergistic effect which enhanced the activity.<sup>29, 35</sup> By comparing with the phase structure and activity of La<sub>1-x</sub>-Sr<sub>x</sub>-Co-O, it is inferred that the presence of both Co<sub>3</sub>O<sub>4</sub> and LaCoO<sub>3</sub> is essential to the reaction, with a preferred ratio at  $x = 0.3$ . At the beginning ( $x \leq 0.3$ ) the increase of Sr content leads to the segregation of Co<sub>3</sub>O<sub>4</sub>, which contributes to the reaction by cooperation with LaCoO<sub>3</sub>, but with the further increase of Sr content ( $x = 0.7$ ) the perovskite structure was destroyed and thus decreased the activity.

To confirm that synergistic effect between the phases occurs, catalytic activity of Co<sub>3</sub>O<sub>4</sub>, La<sub>0.7</sub>Sr<sub>0.3</sub>CoO<sub>3</sub>, La<sub>0.7</sub>-Sr<sub>0.3</sub>-Co-O and a mechanically mixed sample containing 60% Co<sub>3</sub>O<sub>4</sub> and 40% LaCoO<sub>3</sub> (Co<sub>3</sub>O<sub>4</sub>-LaCoO<sub>3</sub>, prepared based on the phase composition of La<sub>0.7</sub>-Sr<sub>0.3</sub>-Co-O) for CO oxidation are tested and compared, Figure 3C. The activity increases in the sequence of La<sub>0.7</sub>Sr<sub>0.3</sub>CoO<sub>3</sub> < Co<sub>3</sub>O<sub>4</sub>-LaCoO<sub>3</sub> < Co<sub>3</sub>O<sub>4</sub> < La<sub>0.7</sub>-Sr<sub>0.3</sub>-Co-O, indicating that the high activity of La<sub>0.7</sub>-Sr<sub>0.3</sub>-Co-O should not be due to a simple overlapping in the activity of LaCoO<sub>3</sub> and Co<sub>3</sub>O<sub>4</sub>, as the physically mixed sample shows low activity for CO oxidation. In other words, a synergistic effect between the phases of La<sub>0.7</sub>-Sr<sub>0.3</sub>-Co-O nano-composite that contributes to the reaction is induced. It is noted that La<sub>0.7</sub>-Sr<sub>0.3</sub>-Co-O shows 96%, while La<sub>0.7</sub>Sr<sub>0.3</sub>CoO<sub>3</sub> shows only 10% CO conversion at temperature below 150 °C, demonstrating clearly the importance of the presence of Co<sub>3</sub>O<sub>4</sub> in the sample.

For CO oxidation catalyzed by perovskite oxides it is generally accepted that the sample with more oxygen vacancy and/or higher metal oxidation state is more favorable for the reaction.<sup>36, 37</sup> Herein, La<sub>0.7</sub>-Sr<sub>0.3</sub>-Co-O with lower surface Co<sup>3+</sup>/Co<sup>2+</sup> and O<sub>ads</sub>/O<sub>latt</sub> ratio (see Table 1) however exhibits higher activity than La<sub>0.7</sub>Sr<sub>0.3</sub>CoO<sub>3</sub>. The reason is that the structure of the former is not totally perovskite, thus the activity is not solely contributed from the perovskite, but from a synergistic effect induced from the multi-phases. The synergistic effect can be verified by the dynamical results obtained from the O<sub>2</sub>-TPD and H<sub>2</sub>-TPR measurements (see Figure S5 of the SI). For example, the oxygen desorption or mobility is more facilitated over La<sub>0.7</sub>-Sr<sub>0.3</sub>-Co-O than that over La<sub>0.7</sub>Sr<sub>0.3</sub>CoO<sub>3</sub>, although the former has lower O<sub>ads</sub>/O<sub>latt</sub> ratio.

The long-time stability of La<sub>0.7</sub>-Sr<sub>0.3</sub>-Co-O composite for CO oxidation reaction was conducted to test if the material benefits from the thermal stability of perovskite oxide. To ensure that the results are reliable, the temperature is controlled at 140 °C with activity of *ca.* 80%. Result in Figure 3D shows that the activity is stable and no appreciable change in the activity is observed even after running for 36 h, indicating that the material has good stability in the reaction. In contrast, a slight decrease in the activity of Co<sub>3</sub>O<sub>4</sub> is observed after 36 h (see Figure S7 of the SI), indicating that the presence of perovskite oxides is essential in stabilizing the catalytic behavior. Characterizations by XRD, XPS and BET confirm that the sample has stable structure (see

Figure S8 of the SI). This directs a way of designing low-temperature active perovskite-based catalyst for CO oxidation.

Table 2. Comparison in the activity (T<sub>ign.</sub>, T<sub>50</sub> and T<sub>100</sub>) of La<sub>0.7</sub>-Sr<sub>0.3</sub>-Co-O with that of LaCoO<sub>3</sub> reported in literature

Entry	Catalyst	T <sub>ign.</sub> (°C) <sup>a</sup>	T <sub>50</sub> (°C) <sup>b</sup>	T <sub>100</sub> (°C) <sup>c</sup>	Refs.
1	La <sub>0.7</sub> -Sr <sub>0.3</sub> -Co-O	75	130	174	This work
2	La-Co-O	100	150	200	This work
3	LaCoO <sub>3</sub> (porous)	60	145	175	15
4	LaCoO <sub>3</sub> (Nano-sized)	100	161	200	38
5	LaCoO <sub>3</sub> (spherical)	70	131	170	38
6	LaCoO <sub>3</sub> (3DOM)	50	162	190	14
7	LaCoO <sub>3</sub>	120	182	215	14
8	LaCoO <sub>3</sub> (porous)	110	170	207	13
9	LaCoO <sub>3</sub>	140	187	237	13
10	La <sub>0.9</sub> K <sub>0.1</sub> CoO <sub>3</sub>	160	245	335	39
11	LaCoO <sub>3</sub>	130	205	246	40
12	LaCoO <sub>3</sub>	160	238	270	41
13	LaCoO <sub>3</sub>	115	172	210	42
14	LaCoO <sub>3</sub>	260	280	400	36

<sup>a</sup> Ignition temperature for CO oxidation; <sup>b</sup> Temperature for 50% CO conversion; <sup>c</sup> Temperature for 100% CO conversion

In order to illuminate the superiority of the La<sub>0.7</sub>-Sr<sub>0.3</sub>-Co-O nano-composite, we compare the activity of CO oxidation over a large number of LaCoO<sub>3</sub> catalysts reported in literature, as listed in Table 2 (for reaction conditions see Table S1 of the SI). La<sub>0.7</sub>-Sr<sub>0.3</sub>-Co-O shows comparable activity to LaCoO<sub>3</sub> prepared with special structures (porous, spherical and 3DOM, see entries 3, 5 and 6) and the activity is higher than that of the others. Considering the easy synthesis procedure and energy savings of La<sub>0.7</sub>-Sr<sub>0.3</sub>-Co-O (the preparation of spherical and 3DOM LaCoO<sub>3</sub> needs special steps and is energy costing, which can be inferred by comparing the preparation procedures), we believe that this sample would be more interesting for future use.

In summary, we report a low-temperature active La<sub>0.7</sub>-Sr<sub>0.3</sub>-Co-O nano-composite for CO oxidation. The sample is prepared by sol-gel method using ethylene glycol and formic acid as complexing agents, and possesses a multi-phase and nano-sized structure. Because of the nano-sized structure and especially the phase cooperation effect, the La<sub>0.7</sub>-Sr<sub>0.3</sub>-Co-O shows improved low-temperature activity for CO oxidation, with the temperature for ignition and 100% CO conversion reached at 70 and 174 °C, respectively. Long-term stability test shows that the sample is stable in the reaction, without appreciable loss in the activity for at least 36 h. The improved catalytic performance and good stability demonstrate that the current strategy of designing nano-sized samples with mixed phases is an effective way to prepare low-temperature active oxides catalyst for CO oxidation in future.

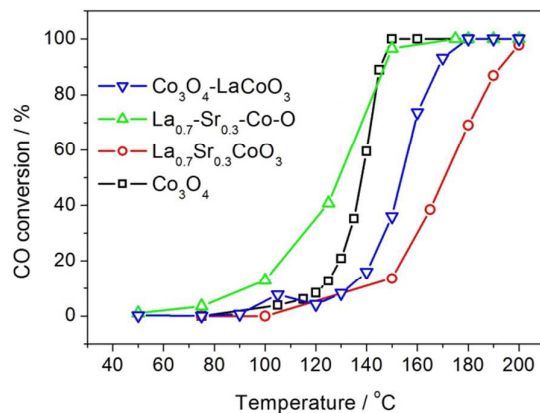
Financial support from the National Science Foundation of China (21203254), the Scientific Research Foundation for Returned Scholars, Ministry of Education of China (BZY11055) and the National Demonstration Center of Experimental Teaching on ethnical pharmacy, South-Central University for Nationalities, is gratefully acknowledged.

## Notes and references

Key Laboratory of Catalysis and Materials Science of the State Ethnic Affairs & Commission Ministry of Education, South-Central University for Nationalities, Wuhan 430074, China; E-mail: ciaczjz@gmail.com

- † Electronic Supplementary Information (ESI) available: Experimental section, additional characterizations and activity tests. See DOI: 10.1039/b000000x/
1. P. Ciambelli, S. Cimino, S. De Rossi, M. Faticanti, L. Lisi, G. Minelli, I. Pettiti, P. Porta, G. Russo and M. Turco, *Appl. Catal. B: Environ.*, 2000, 24, 243-253.
  2. M. Misono, *Stud. Surf. Sci. Catal.*, 2013, 176, 67-95.
  3. M. A. Pena and J. L. G. Fierro, *Chem. Rev.*, 2001, 101, 1981-2017.
  4. N. Yamazoe and Y. Teraoka, *Catal. Today*, 1990, 8, 175-199.
  5. Y. Nishihata, J. Mizuki, T. Akao, H. Tanaka, M. Uenishi, M. Kimura, T. Okamoto and N. Hamada, *Nature*, 2002, 418, 164-167.
  6. J. J. Zhu and A. Thomas, *Appl. Catal. B: Environ.*, 2009, 92, 225-233.
  7. C. H. Kim, G. Qi, K. Dahlberg and W. Li, *Science*, 2010, 327, 1624-1627.
  8. J. Zhu, H. Li, L. Zhong, P. Xiao, X. Xu, X. Yang, Z. Zhao and J. Li, *ACS Catal.*, 2014, 4, 2917-2940.
  9. H. X. Dai, H. He, W. Li, Z. Z. Gao and C. T. Au, *Catal. Lett.*, 2001, 73, 149-156.
  10. U. G. Singh, J. Li, J. W. Bennett, A. M. Rappe, R. Seshadri and S. L. Scott, *J. Catal.*, 2007, 249, 349-358.
  11. H. Taguchi, S. Yamasaki, A. Itadani, M. Yosinaga and K. Hirota, *Catal. Commun.*, 2008, 9, 1913-1915.
  12. W. Yang, R. Zhang, B. Chen, N. Bion, D. Duprez and S. Royer, *J. Catal.*, 2012, 295, 45-58.
  13. Y. Wang, X. Cui, Y. Li, Z. Shu, H. Chen and J. Shi, *Micropor. Mesopor. Mater.*, 2013, 176, 8-15.
  14. X. Li, H. Dai, J. Deng, Y. Liu, S. Xie, Z. Zhao, Y. Wang, G. Guo and H. Arandiyán, *Chem. Eng. J.*, 2013, 228, 965-975.
  15. P. Xiao, J. Zhu, H. Li, W. Jiang, T. Wang, Y. Zhu, Y. Zhao and J. Li, *ChemCatChem*, 2014, 6, 1774-1781.
  16. X. W. Xie, Y. Li, Z. Q. Liu, M. Haruta and W. J. Shen, *Nature*, 2009, 458, 746-749.
  17. Y. Lv, Y. Li and W. Shen, *Catal. Commun.*, 2013, 42, 116-120.
  18. K. Qian, L. Luo, H. Bao, Q. Hua, Z. Jiang and W. Huang, *Catal. Sci. Technol.*, 2013, 3, 679-687.
  19. M. Haruta, T. Kobayashi, H. Sano and N. Yamada, *Chem. Lett.*, 1987, 405-408.
  20. G. Pecchi, P. Reyes, R. Zamora, C. Campos, L. E. Caduus and B. P. Barbero, *Catal. Today*, 2008, 133, 420-427.
  21. C. Zhang, Y. Guo, Y. Guo, G. Lu, A. Boreave, L. Retailleau, A. Baylet and A. Giroir-Fendler, *Appl. Catal. B: Environ.*, 2014, 148-149, 490-498.
  22. N. A. Merino, B. P. Barbero, P. Ruiz and L. E. Cadús, *J. Catal.*, 2006, 240, 245-257.
  23. C. Zhang, W. Hua, C. Wang, Y. Guo, Y. Guo, G. Lu, A. Baylet and A. Giroir-Fendler, *Appl. Catal. B: Environ.*, 2013, 134-135, 310-315.
  24. C. A. Chagas, F. S. Toniolo, R. N. S. H. Magalhães and M. Schmal, *Int. J. Hydrogen. Energ.*, 2012, 37, 5022-5031.
  25. J. Xu, J. Liu, Z. Zhao, J. Zheng, G. Zhang, A. Duan and G. Jiang, *Catal. Today*, 2010, 153, 136-142.
  26. Y. G. Wang, J. W. Ren, Y. Q. Wang, F. Y. Zhang, X. H. Liu, Y. Guo and G. Z. Lu, *J. Phys. Chem. C*, 2008, 112, 15293-15298.
  27. V. C. Belessi, A. K. Ladavos and P. J. Pomonis, *Appl. Catal. B: Environ.*, 2001, 31, 183-194.
  28. Y. J. Zhu, D. Wang, F. L. Yuan, G. Zhang and H. G. Fu, *Appl. Catal. B: Environ.*, 2008, 82, 255-263.
  29. J. Kirchnerova, M. Alifanti and B. Delmon, *Appl. Catal. A-Gen.*, 2002, 231, 65-80.
  30. V. C. Belessi, C. N. Costa, T. V. Bakas, T. Anastasiadou, P. J. Pomonis and A. M. Efstathiou, *Catal. Today*, 2000, 59, 347-363.
  31. J. Deng, L. Zhang, H. Dai, H. He and C. T. Au, *Ind. Eng. Chem. Res.*, 2008, 47, 8175-8183.
  32. N. Yamazoe, Y. Teraoka and T. Seiyama, *Chem. Lett.*, 1981, 1767-1770.
  33. A. Machocki, T. Ioannides, B. Stasinska, W. Gac, G. Avgouropoulos, D. Delimaris, W. Grzegorzczak and S. Pasieczna, *J. Catal.*, 2004, 227, 282-296.
  34. Y. Yokoi and H. Uchida, *Catal. Today*, 1998, 42, 167-174.
  35. L. Simonot, F. o. Garin and G. Maire, *Appl. Catal. B: Environ.*, 1997, 11, 167-179.
  36. B. Seyfi, M. Baghalha and H. Kazemian, *Chem. Eng. J.*, 2009, 148, 306-311.
  37. K. Rida, A. Benabbas, F. Bouremmad, M. A. Peña and A. Martínez-Arias, *Catal. Commun.*, 2006, 7, 963-968.
  38. Y. Liu, H. Dai, J. Deng, L. Zhang, Z. Zhao, X. Li, Y. Wang, S. Xie, H. Yang and G. Guo, *Inorg. Chem.*, 2013, 52, 8665-8676.
  39. Q. Thi Hoang Yen, T. Thi Minh Nguyet, T. Que Chi, N. Quoc Trung, N. Thi Toan and L. Dang Khuong, *Adv. Nat. Sci.: Nanosci. Nanotechnol.*, 2011, 2, 045007.
  40. S. Sun, L. Yang, G. Pang and S. Feng, *Appl. Catal. A: Gen.*, 2011, 401, 199-203.
  41. S. A. Nedil'ko, I. V. Fesich, A. G. Dzyaz'ko, O. Z. Didenko, G. R. Kosmambetova and P. E. Strizhak, *Theor. Exp. Chem.*, 2011, 47, 183-187.
  42. P. Doggali, S. Kusaba, Y. Teraoka, P. Chankapure, S. Rayalu and N. Labhsetwar, *Catal. Commun.*, 2010, 11, 665-669.

## Graphical Abstract



$\text{La}_{0.7}\text{Sr}_{0.3}\text{Co-O}$  nano-composite shows improved catalytic activity to CO oxidation relative to  $\text{La}_{0.7}\text{Sr}_{0.3}\text{CoO}_3$  and  $\text{Co}_3\text{O}_4$ , which is suggested to be due to a synergistic effect induced by the phase cooperation.